J. Fluid Mech. (1995), *vol.* 285, *pp.* 1–16

Inertial effects in chaotic mixing with diffusion

By PRADIP DUTTA AND RENE CHEVRAY
Department of Mechanical Engineering, Columbia University, New York, NY 10027, USA

(Received 20 December 1993 and in revised from 15 July 1994)

The role of diffusion and transient velocities in the dispersal of passive scalars by chaotic advection produced in a low Reynolds number periodic journal-bearing flow is studied numerically and experimentally. The transient velocity field, which occurs whenever the cylinders switch motion, is obtained by solving the Navier–Stokes equations numerically in the eccentric annulus. It is observed, numerically, that the transient effects, along with diffusion, significantly enhance the separation of chaotically advected particles even when the Reynolds number is very low. Corresponding experimental observations are found to be in good qualitative agreement with the numerical results obtained by including the effect of transient velocities, which are seen to add to the overall separation of particles.

1. Introduction

It is now well established that seemingly simple low-dimensional dynamical systems, conservative or dissipative, can exhibit sensitive dependence on initial conditions, which consequently produce complicated phase trajectories. Such behaviour is often referred to as *deterministic chaos* (Schuster 1984). These current ideas of nonlinear dynamics have recently been applied to real fluid dynamical systems also. This process can be studied using the Lagrangian description of fluid mechanics, i.e. by following individual fluid particle trajectories. A system of partial differential equations (i.e. the Navier–Stokes equations) describe the evolution of a system's velocity field, but the particle trajectories are governed by ordinary differential equations of the form

$$\dot{x} = u(x, y, z, t), \quad \dot{y} = v(x, y, z, t), \quad \dot{z} = w(x, y, z, t), \tag{1a–c}$$

where the velocity field components u, v, and w may or may not be known explicitly. Chaotic advection occurs when highly complicated particle trajectories are observed in the Lagrangian frame of reference even for simple well-behaved velocity fields.

Aref (1984) made the fundamental observation that the streamfunction, ψ, in two-dimensional incompressible flows plays the role of a Hamiltonian in classical mechanics:

$$\dot{x} = \frac{\partial \psi}{\partial y}, \quad \dot{y} = -\frac{\partial \psi}{\partial x}. \tag{2}$$

Thus, in terms of dynamical systems, ψ plays the role of a Hamiltonian, and x, y are canonically conjugate phase-space variables. For a time-independent ψ, the system of equations (2) constitutes a single-degree-of-freedom dynamical system in which the orbits lie on smooth curves in the x, y phase plane. In terms of fluid mechanics, this situation corresponds to a steady flow in which the fluid particles move along the streamlines. However, if ψ is time dependent, it is possible for the system to exhibit chaotic particle trajectories.

The required time dependence of the streamfunction need not necessarily be due to the effects of high Reynolds number flows in which the velocities fluctuate stochastically, but may be caused by some simple, external modulation of the flow system. Idealized models demonstrating chaotic advection include a point vortex model of Aref (1984), tendril–whorl flow of Khakhar, Franjione & Ottino (1987), and a pulsed source–sink system of Jones & Aref (1988). Amongst physically realizable models, the periodically driven cavity flow and the journal bearing flow are the most common. Chaotic mixing in periodically driven two-dimensional cavity flows has been studied by several authors, including Khakhar & Ottino (1985), Chien, Rising & Ottino (1986), Leong & Ottino (1989), and Liu & Peskin (1991). In the journal bearing system, which consists of two eccentric cylinders, the annular region is filled with a viscous liquid and the cylinders are rotated alternately to produce chaotic advection. Chaiken *et al.* (1986) studied this system experimentally as well as numerically to produce chaotic advection in a Stokes flow between the cylinders. Similar simultaneous numerical studies were reported by Aref & Balachandar (1986). A detailed comparison of experimental and numerical results for the case of chaotic mixing in a journal bearing flow is reported in Swanson & Ottino (1990). In the same geometry, studies on material line stretching and drop breakup have also been reported (Muzzio & Swanson, 1991; Muzzio *et al.* 1992; Tjahjadi, Stone & Ottino 1992). The effect of molecular diffusion in chaotic mixing was investigated by Aref & Jones (1989) who performed numerical experiments to show that diffusion significantly enhances the separation of particles in a non-integrable Stokes flow. Further investigations with diffusion are reported by the present authors (Dutta & Chevray 1991) and by Jones (1991).

In the above studies, with or without diffusion, the numerical work was carried out with a Stokes flow assumption for the deterministic velocity. In other words, it was assumed that the flow in the eccentric annulus produced by periodic rotation of the cylinders is free from inertia effects and is piecewise steady. The transient and inertia terms from the momentum equations were omitted following the rationale that, for a low Reynolds number flow within Stokes regime, they are negligible in comparison to the viscous terms. Although in Dutta & Chevray (1991) numerical predictions (using a Stokes flow assumption) of separation of diffusive particles were qualitatively verified by experimental observations for a few cycles of stirring, comparisons for higher number of cycles of stirring in a flow reversibility experiment could not be successfully performed because of observed deviations of the numerical results from the experimental ones. Chaiken *et al.* (1986), too, report the poor reversibility of a blob of particles initialized in a chaotic region during a flow reversibility experiment. It is believed here that the deviation is because of the omission of diffusion and transient effects in their numerical formulation. The transient effects, which occur in a periodic journal bearing flow when the cylinders switch motions, last only for a few seconds. Although the transient time is very small compared to the cylinder rotation time in a cycle (which is of the order of a few minutes), the transient effects may be significant in a chaotic region where the particles are sensitive even to small displacements. This effect is studied here first by obtaining a numerical solution of the time-dependent Navier–Stokes equation, and then using the flow solution to study the separation of a blob of particles. The results are then compared with experimental observations.

2. Numerical studies

2.1. *Diffusion in a Lagrangian frame of reference*

To model the Lagrangian description of a diffusing particle, the generalized Langevin equation is used:

$$\frac{\mathrm{d}\boldsymbol{x}}{\mathrm{d}t} = \boldsymbol{V}(\boldsymbol{x}, t) + \boldsymbol{S}(t), \tag{3}$$

where $\boldsymbol{x}(t)$ is the position of a diffusing particle, $\boldsymbol{V}(\boldsymbol{x}, t)$ is the deterministic velocity as a result of the flow solution, and $\boldsymbol{S}(t)$ is the stochastic component arising out of the Brownian motion of the molecules. Similar models were also used by Aref & Jones (1989). Herein, a distinction must be made between chaotic processes, which are low-dimensional dynamical systems, and stochastic processes, such as molecular diffusion, which are random.

$\boldsymbol{S}(t)$ is assumed to be a Gaussian process with zero mean and variance proportional to the diffusivity, D. In other words,

$$\left.\begin{aligned} \langle \boldsymbol{S}(t) \rangle &= 0, \\ \langle \boldsymbol{S}(t)\, \boldsymbol{S}(t') \rangle &= 2D\delta_{ij}\, \delta(t-t'). \end{aligned}\right\} \tag{4}$$

If $\boldsymbol{V}(\boldsymbol{x}, t)$ in (3) is explicitly known, and $\boldsymbol{S}(t)$ is modelled as described above, then (3) can be integrated with time to obtain the position of the diffusing particle at any time. $\boldsymbol{V}(\boldsymbol{x}, t)$ can be obtained by solving the continuity equation

$$\nabla \cdot \boldsymbol{V} = 0 \tag{5}$$

and the momentum equation (assuming incompressible Newtonian fluid)

$$\rho \frac{\mathrm{D}\boldsymbol{V}}{\mathrm{D}t} = -\nabla p + \mu \nabla^2 \boldsymbol{V}, \tag{6}$$

where ρ is the density of the fluid and μ is the dynamic viscosity.

2.2. *Numerical solution of the Navier–Stokes equations*

Since chaotically advected particles are very sensitive to initial conditions, transient and inertia effects may become significant above a certain Reynolds number, especially when there is flow reversal and taking particle diffusion into account. To study this effect, $\boldsymbol{V}(\boldsymbol{x}, t)$ is obtained by solving the full Navier–Stokes equations numerically with the appropriate boundary conditions.

For an incompressible Newtonian fluid with constant properties the governing equations of motion in a two-dimensional Cartesian coordinate system are

continuity:
$$\frac{\partial u}{\partial x} + \frac{\partial v}{\partial y} = 0; \tag{7}$$

momentum:
$$\frac{\partial u}{\partial t} + u\frac{\partial u}{\partial x} + v\frac{\partial u}{\partial y} = -\frac{1}{\rho}\frac{\partial p}{\partial x} + \nu\left(\frac{\partial^2 u}{\partial x^2} + \frac{\partial^2 u}{\partial y^2}\right), \tag{8a}$$

$$\frac{\partial v}{\partial t} + u\frac{\partial v}{\partial x} + v\frac{\partial v}{\partial y} = -\frac{1}{\rho}\frac{\partial p}{\partial y} + \nu\left(\frac{\partial^2 v}{\partial x^2} + \frac{\partial^2 v}{\partial y^2}\right). \tag{8b}$$

The above equations are solved for an eccentric annular region with no-slip boundary conditions on the inner and outer cylinder surfaces. In order to solve the above governing equations numerically using a finite difference technique, it is

appropriate to perform a suitable coordinate transformation so that the computation can be done in a rectangular domain. The bipolar coordinate system has in the past been applied to solve conveniently engineering probelms concerning eccentric annulus (e.g. Cho, Chang & Park 1982). Here, we have performed the computations by transforming the governing equations and the boundary conditions from the Cartesian coordinate system (x, y) to a bipolar system (ξ, η). The transformation is as follows:

$$x = -b\frac{\sinh\xi}{\cosh\xi - \cos\eta}, \quad y = b\frac{\sin\eta}{\cosh\xi - \cos\eta}, \tag{9}$$

where b is a positive number.

For a two-dimensional incompressible flow, we define the streamfunction, ψ, in Cartesian coordinates as

$$u = \frac{\partial\psi}{\partial y}, \quad v = -\frac{\partial\psi}{\partial x} \tag{10}$$

and vorticity, ς, as

$$\varsigma = \frac{\partial u}{\partial y} - \frac{\partial v}{\partial x}. \tag{11}$$

Using (10) and (11) in our governing equations (7) and (8), and carrying out the transformation shown in (9), we get the streamfunction–vorticity formulation in bipolar coordinates as

$$-\varsigma = \left(\frac{\cosh\xi - \cos\eta}{b}\right)^2 \left(\frac{\partial^2\psi}{\partial\xi^2} + \frac{\partial^2\psi}{\partial\eta^2}\right), \tag{12}$$

$$\frac{\partial\varsigma}{\partial t} + \left(\frac{\cosh\xi - \cos\eta}{b}\right)^2 \frac{\partial\psi}{\partial\eta}\frac{\partial\varsigma}{\partial\xi} - \left(\frac{\cosh\xi - \cos\eta}{b}\right)^2 \frac{\partial\psi}{\partial\xi}\frac{\partial\varsigma}{\partial\eta} = \nu\left(\frac{\cosh\xi - \cos\eta}{b}\right)^2 \left(\frac{\partial^2\varsigma}{\partial\xi^2} + \frac{\partial^2\varsigma}{\partial\eta^2}\right), \tag{13}$$

with the transformed boundary conditions

$$\left.\begin{aligned} &\psi(\xi_o, \eta, t) = 0 \\ &\frac{\partial\psi}{\partial\xi}(\xi_o, \eta, t) = -\Omega_o R_o\left(\frac{b}{\cosh\xi_o - \cos\eta}\right) \end{aligned}\right\} \quad \text{on the outer cylinder,} \tag{14a}$$

and

$$\left.\begin{aligned} &\psi(\xi_i, \eta, t) = Q(t) \\ &\frac{\partial\psi}{\partial\xi}(\xi_i, \eta, t) = -\Omega_i R_i\left(\frac{b}{\cosh\xi_i - \cos\eta}\right) \end{aligned}\right\} \quad \text{on the inner cylinder,} \tag{14b}$$

where ξ_i and ξ_o represent the inner and outer cylinders, respectively; Ω_i and Ω_o the angular velocities of the inner and outer cylinders, respectively; and $Q(t)$ the volume flow rate between the two cylinders. The initial conditions are $\psi = 0$ and $\varsigma = 0$ everywhere when the fluid starts from rest. When motion is being switched from one cylinder to the other, however, the initial conditions are given by the vorticity distribution at the end of the previous motion.

In order to apply a finite difference method to solve the differential equations (12) and (13), the domain is discretized as shown in figure 1. The solution of the transient vorticity transport equation (13) is obtained by using an alternate direct implicit method. Simultaneous solution of the streamfunction equation (12) is obtained using the Gauss–Siedel iterative method with successive over-relaxation to increase the speed of convergence.

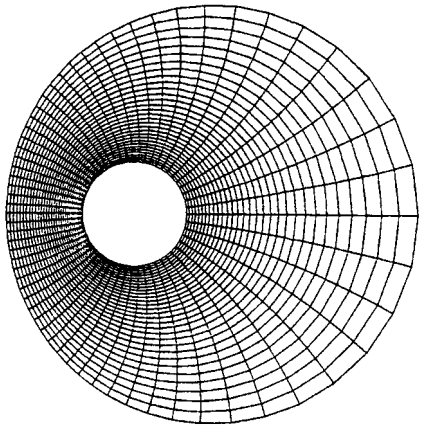

FIGURE 1. Discretization by a (31 × 61) grid of the physical domain.

2.3. *Integration of particle paths*

Since our prime objective is to follow a particle in a Lagrangian frame for a flow field which includes the transient velocities, we must store the velocity values at every grid point for various time steps while the flow is developing. Once the flow attains a steady state in a given cycle, we store just one set of velocity values for that entire steady state. But when the cylinders switch motion, the flow becomes unsteady again, and we must store the values at various time steps until the flow becomes fully developed again.

With a Stokes flow assumption, there are analytical solutions available for the geometry in question (e.g. Ballal & Rivlin 1977). As a result, in all previous studies the integration of the particle positions could easily be found by employing standard techniques such as the Runge–Kutta method using the known value of the velocity at every location. On the other hand, for the numerical solution which we now have, the velocity values are available only at the grid point locations. In most cases, the particle will lie outside any grid point in a region surrounded by four grid points. The velocity at a particular location (x, y) is determined using an appropriate interpolation method. In this study, we have chosen the bilinear interpolation which makes use of the dependent variable only at the four neighbouring nodes. This method is quick, and it is accurate if we have sufficiently dense grid points and if the nonlinear terms of the momentum equations are small (i.e. if the Reynolds number is not too high).

2.4. *Poincaré sections*

After initializing a fluid particle at any location in the eccentric annular region, its position can be determined at any later time by integrating the deterministic velocity solution, $\boldsymbol{V}(\boldsymbol{x}, t)$, with respect to time. Defining each pair of rotations (one by the inner cylinder with the outer stationary, and one by the outer with the inner stationary) as a 'cycle', the particle position can be viewed and recorded at the end of each cycle (i.e. at $t = 0, T, 2T, \ldots, nT$, where T is the time period of each cycle of motion, and n is the total number of iterations). Such plotting of particle positions can be done by initializing the particles of various 'key' locations inside the annular region, and the resulting plot becomes a *Poincaré section* or *surface of section*. Poincaré maps for the journal bearing flow system have been constructed by Tan (1985) and Chaiken *et al.* (1986) for a variety of cylinder eccentricities and angular displacements. These maps, depending on the system parameter values, reveal a rich mixture of regular and chaotic particle motions. A typical example is shown in figure 2 in which the *chaotic regions*

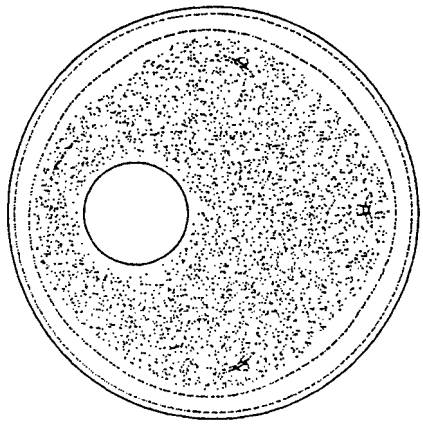

FIGURE 2. Poincaré surfaces-of-section produced with a Stokes flow assumption of the velocity field with inner cylinder radius $R_i = 0.25$, outer cylinder radius $R_o = 1.0$. (Dimensions normalized with respect to outer cylinder radius.) Eccentricity is $0.375R_o$, and each cycle comprises 0.875 revolutions of the inner cylinder (counterclockwise) followed by 0.3 revolutions of the outer cylinder (counterclockwise).

correspond to the ones filled with dots randomly distributed, while the *regular regions* are marked by closed curves.

2.5. *Numerical experiments*

The objective of the present research is to study the effects of diffusion and transient velocities on the overall mixing of the particles in a chaotically advected flow. Transients velocities prevail when the cylinders switch motions. The numerical investigation is carried out by locating circular blobs of particles in a chosen chaotic region of a given phase space. Each blob is represented by about 2000 evenly distributed points inside a small circle. With a given value of the diffusivity, D, the two-cylinder system is stirred numerically using (3) by completing a few cycles of motion followed by the same number of reverse cycles. If the particle motions are deterministic (i.e. if $D = 0$ and transient effects are neglected), the particles return to their initial locations after flow reversal. (This would be true if we were to stir the system only for a finite number of cycles, thus preventing the numerical errors building up.) But with a finite D and/or if the transient effects are taken into account, the particles are no longer expected to return to their initial locations after flow reversal, even for a few cycles of stirring. At the end of the flow reversal, the mean-square separation, σ^2, of the particles from their initial locations is evaluated by the following equation:

$$\sigma^2 = \frac{1}{N}\sum_{n=1}^{N}(x_i - x_f)_n^2, \tag{15}$$

where the subscripts i and f refer to the initial and final positions, respectively, and N is the total number of particles. Individual effects of diffusion, transients, and their combined effect on the separation of particles are studied for a variety of blob initializations and stirring time.

3. Experimental arrangement

The apparatus constructed is shown schematically in figure 3. Both cylinders are made of Plexiglas, with the outer one being hollow, while the inner one is solid. The axes of both cylinders are vertical. The physical dimensions are shown in figure 3. The

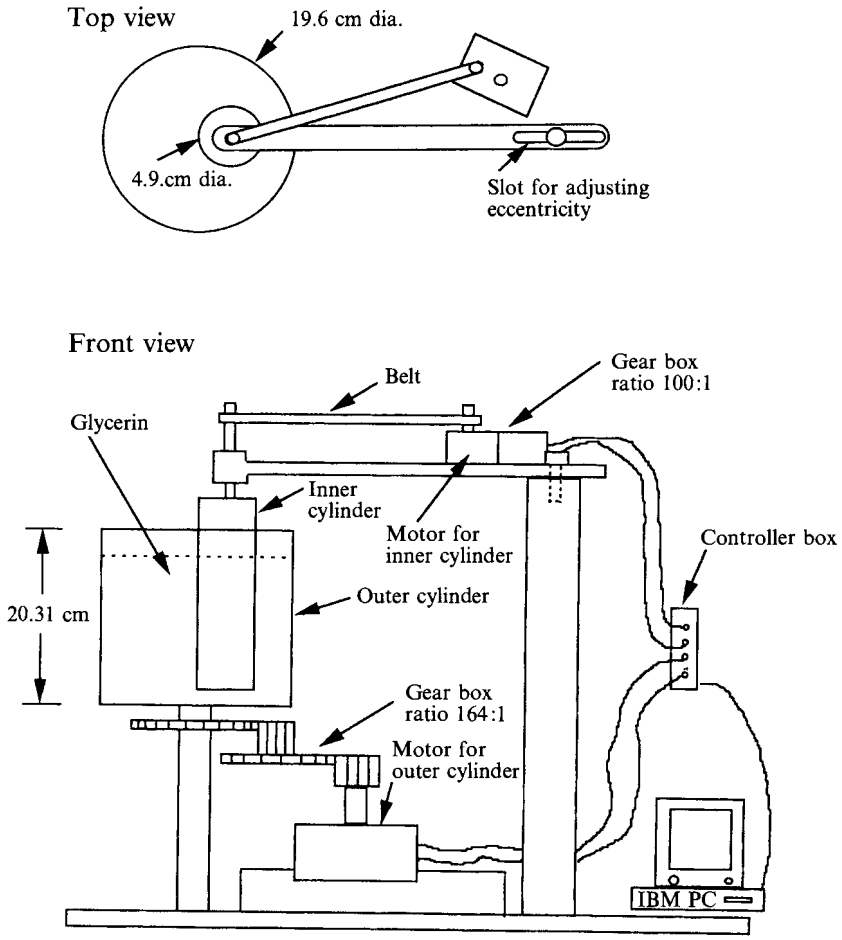

FIGURE 3. Schematic diagram of the experimental arrangement.

cylinders are made long enough so that the effect of the bottom surface can be neglected as long as the tracers are introduced close to the upper surface. In order to adjust the eccentricity of the cylinders, the inner cylinder is attached to a horizontal strut which can move in a horizontal slot.

The working fluid is chosen to be glycerin because it is clear, is miscible with water, has a Newtonian behaviour, and has sufficiently high viscosity so that the Reynolds number remains very low (within Stokes regime, if the rotational speeds are low enough). The Reynolds number, Re, is defined as

$$\mathrm{Re} = \frac{\rho[R_i \Omega(R_o - R_i)]}{\mu}, \tag{16}$$

where R_i and R_o are the radii of the inner and outer cylinders respectively, and Ω is the angular velocity. Dye solution is prepared by dissolving a small amount of fluorescent powder in glycerin. The dye is thus made neutrally buoyant in the fluid so as to prevent any three-dimensional effect.

The flow between the two cylinders is modulated by rotating the cylinders in the desired fashion by means of two stepper motors, one connected to each cylinder. The precise control of the rotation rate, direction, and the angular displacement of each

motor per cycle is achieved with the help of a personal computer. The heart of the experimental set-up is a driver system (consisting of two stepper motors with drivers and controller boards) which controls the rotations of the two cylinders precisely. The motor driver can deliver between 50 and 500 steps per second to the motor and each step rotates the motor by 1.8°. Speed reduction is achieved by means of a gear train such that the rotational speed of each cylinder can be as low as 0.1 r.p.m.

The procedure followed in the experiments is similar to the one used in the numerical experiments. First, a set of flow parameters is chosen which can produce the desired Poincaré section. From the corresponding Poincaré map, the regions of chaotic and regular behaviour can be identified. For comparison, the flow parameters chosen for experiments are made to match those used for numerical studies. Using a 25-gauge hypodermic needle, a circular blob of dye is introduced just below the fluid surface.

The dye is illuminated by ultraviolet light and it is photographed by a camera fixed just above the apparatus. Ultraviolet light is used because it makes only the fluorescent dye glow. Further, in order to prevent any reflection from the cylinders, the inner cylinder and the bottom of the outer cylinder are painted black. The two-cylinder system is then stirred for a few cycles of motion and another photograph is taken at the end of the forward cycles. An equal number of reverse cycles are then performed and, at the end of the reverse cycles, a final photograph of the blob is taken.

4. Results and discussion

4.1. *Testing the accuracy of the numerical solution*

Before examining the irreversibility caused by transient effects, the numerical accuracy of the flow solution and the associated interpolation method for integration of particle paths must be verified. First, we obtain a numerical solution of the velocity field using a cylinder rotation speed of 0.1 r.p.m., which corresponds to a Reynolds number within the Stokes regime. Next, we construct a Poincaré section using piecewise steady numerical solutions of the velocity field (figure 4). It is found to be in excellent agreement with corresponding ones obtained using analytical solution of the Stokes flow (figure 2). This demonstrates that the numerical solution and the associated interpolation technique is able to capture the same details of the Poincaré mapping as produced by the analytical solutions, and is therefore suitable for the study of chaotic advection.

Next, we estimate the order of magnitude of the numerical error accumulated while numerically integrating the particle positions with time. This is done by performing the following numerical experiments regarding separation of a blob of particles. Using piecewise steady velocity fields, and setting $D = 0$ in equation (3), the system is stirred for a few cycles of motion followed by an equal number of reverse cycles. The flow parameters chosen correspond to those of figure 2, and the blob initialization is shown in figure 5(*a*). At the end of the flow reversal, the mean square separation, σ^2, of the particles from their initial locations is evaluated according to equation (15). Ideally, in the absence of any numerical error, the particles would come back to their initial locations at the end of the reverse cycles, and σ^2 would be zero. For the grid system chosen, the flow reversal experiment with ten cycles gave a maximum σ^2 of the order of 10^{-10} m^2. Since the diameter of the outer cylinder is about 0.2 m, this indicates a reasonable degree of accuracy of our numerical solutions. This method was used to validate the choice of grid sizes for the numerical solution of the Navier–Stokes equations. For a higher number of cycles of stirring, one may need more numerical accuracy for the calculation of the velocity field, which would then necessitate the

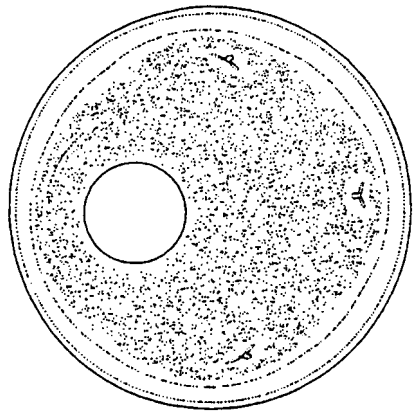

FIGURE 4. Poincaré section obtained by using piecewise steady flow solution (i.e. without transient effects) using the numerical solution of Navier–Stokes flow with Reynolds number within the Stokes regime. The flow parameters are as in figure 2.

choice of a finer mesh. But for about ten cycles, the present choice of 31×61 grids has proved to be accurate enough.

4.2. *Separation of particles by transient effects*

Next, numerical studies similar to the above were performed, but this time using the transition solution of the velocity field instead of the piecewise steady one. Figure 5 shows the case in which the particles are advected with a cylinder rotational speed of 0.1 r.p.m. The particles in this case, which are advected for 7 and 10 forward cycles, followed by the same number of reverse cycles, do not return to their initial positions. Since the value of D is chosen to be zero (i.e. no diffusion effects), and it was checked earlier that the irreversibility caused by numerical errors was negligible, the principal cause of irreversibility should, therefore, be the transient effects.

In order to enhance the transient effects further, the above numerical experiments were repeated with a cylinder rotational speed of 1.0 r.p.m. which gave a higher Reynolds number, equal to 0.45, above the Stokes flow limit. The corresponding results, shown in figure 6, mark a significant increase of irreversibility after the reverse cycles, which is expected since the inertia is higher and the transients last longer. This time, however, the particle distribution is different from that of the piecewise steady case even after the forward cycles.

4.3. *Separation due to molecular diffusion*

The separation caused by random perturbations such as molecular diffusion is also studied. Suppressing any transient effects (i.e. using the piecewise steady flow solution), and choosing a finite D equal to 5×10^{-12} m^2 s^{-1}, the above numerical experiments were repeated and the separation after flow reversal is evaluated (figure 7). The separation in this case is due only to diffusion effects, since the transient velocities are not taken into account. These calculations are performed in order to compare the magnitude of the two effects separately; the combined effects of diffusion and transient velocities are presented next.

4.4. *Combined effects of transients and diffusion*

Simultaneous consideration of diffusion and transients would simulate a real (experimental) phenomenon more accurately since, in real experiments, both processes take place together. For comparison, the flow parameters in both the numerical work

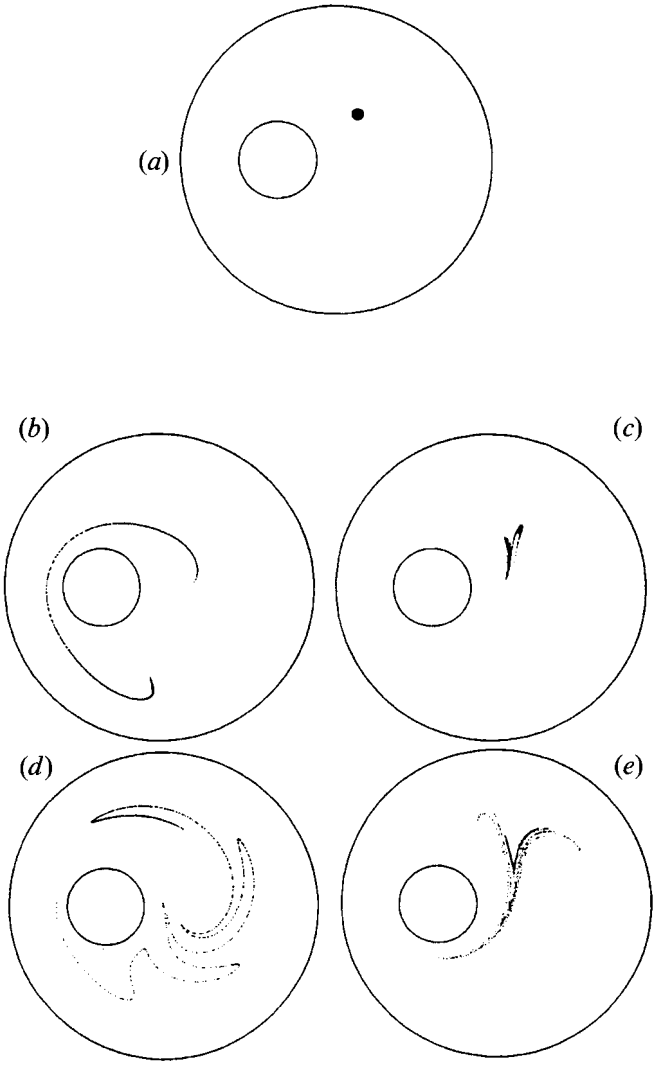

FIGURE 5. Numerical experiments for estimating the separation due to transient effects while stirring in a chaotic region. The flow parameters correspond those of figure 2, and $D = 0$. A transient velocity field with a cylinder speed of 0.1 r.p.m. is used. (*a*) Initial distribution of particles, (*b*) after 7 forward cycles, (*c*) after flow reversal, (*d*) after 10 forward cycles, and (*e*) after flow reversal.

and the experiments are chosen to be identical. The diffusivity, D, in the numerical work is taken to be $5 \times 10^{-12}\ \mathrm{m^2\ s^{-1}}$, which is about the measured value of the diffusivity of the dye in glycerin. The rotational speed of the cylinders in the experiments is chosen to be 0.1 r.p.m., which corresponds to a Reynolds number of 0.045. This keeps the Reynolds number within the Stokes regime. Also, the blob is introduced at a location corresponding to that used in the numerical experiments.

Numerical results and corresponding experimental observations are shown in figures 8 and 9 for 7 and 10 cycles of stirring, respectively. The agreement is remarkable even for 10 cycles of stirring. Such an agreement could not have been obtained earlier with a Stokes solution of the velocity field. This result, however, does not put the Stokes flow assumption under question altogether, because it is still effective in predicting the particle distribution during the forward cycles if the Reynolds number in the

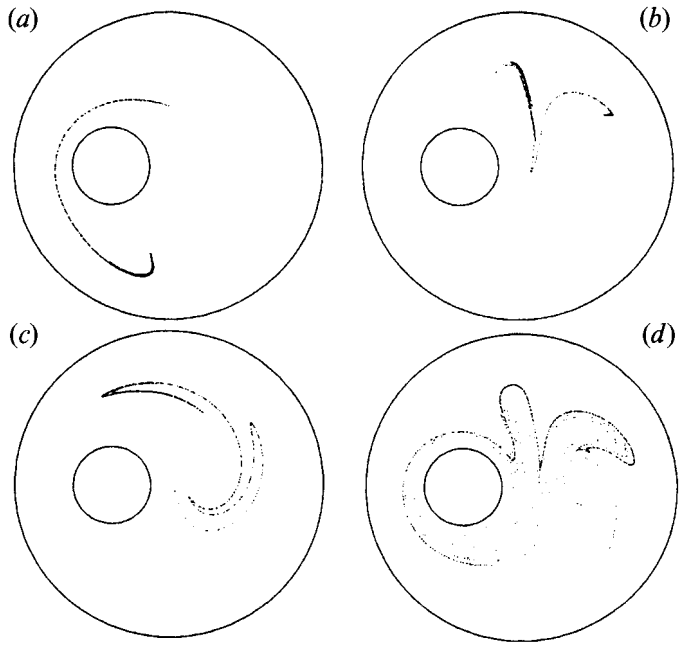

FIGURE 6. As figure 5 but with a cylinder speed of 1 r.p.m. is used. The initial distribution of particles is as in figure 5(*a*). (*a*) After 7 forward cycles, (*b*) after flow reversal, (*c*) after 10 forward cycles, and (*d*) after flow reversal.

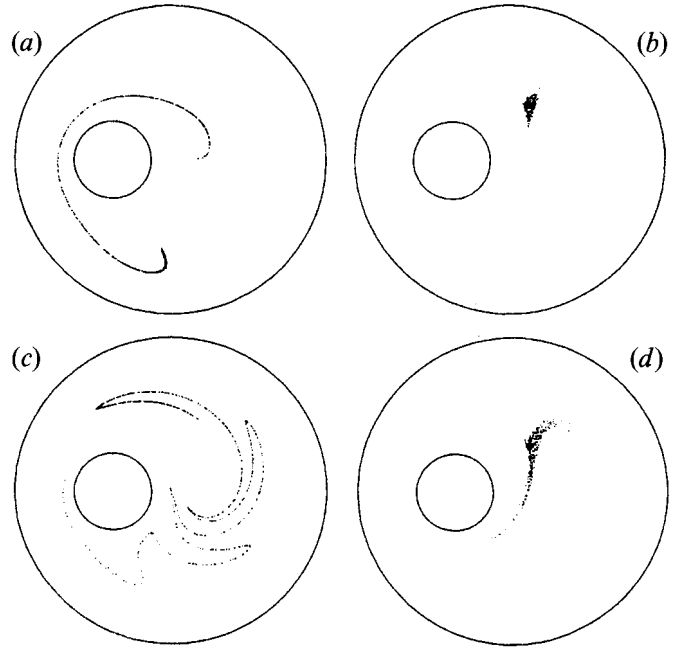

FIGURE 7. Separation due to diffusion effects (no transient effects taken into account) while stirring in a chaotic region. The flow parameters correspond those of figure 2, and $D = 5 \times 10^{-12}$. The initial distribution of particles is as in figure 5(*a*). (*a*) After 7 forward cycles, (*b*) after flow reversal, (*c*) after 10 forward cycles, and (*d*) after flow reversal.

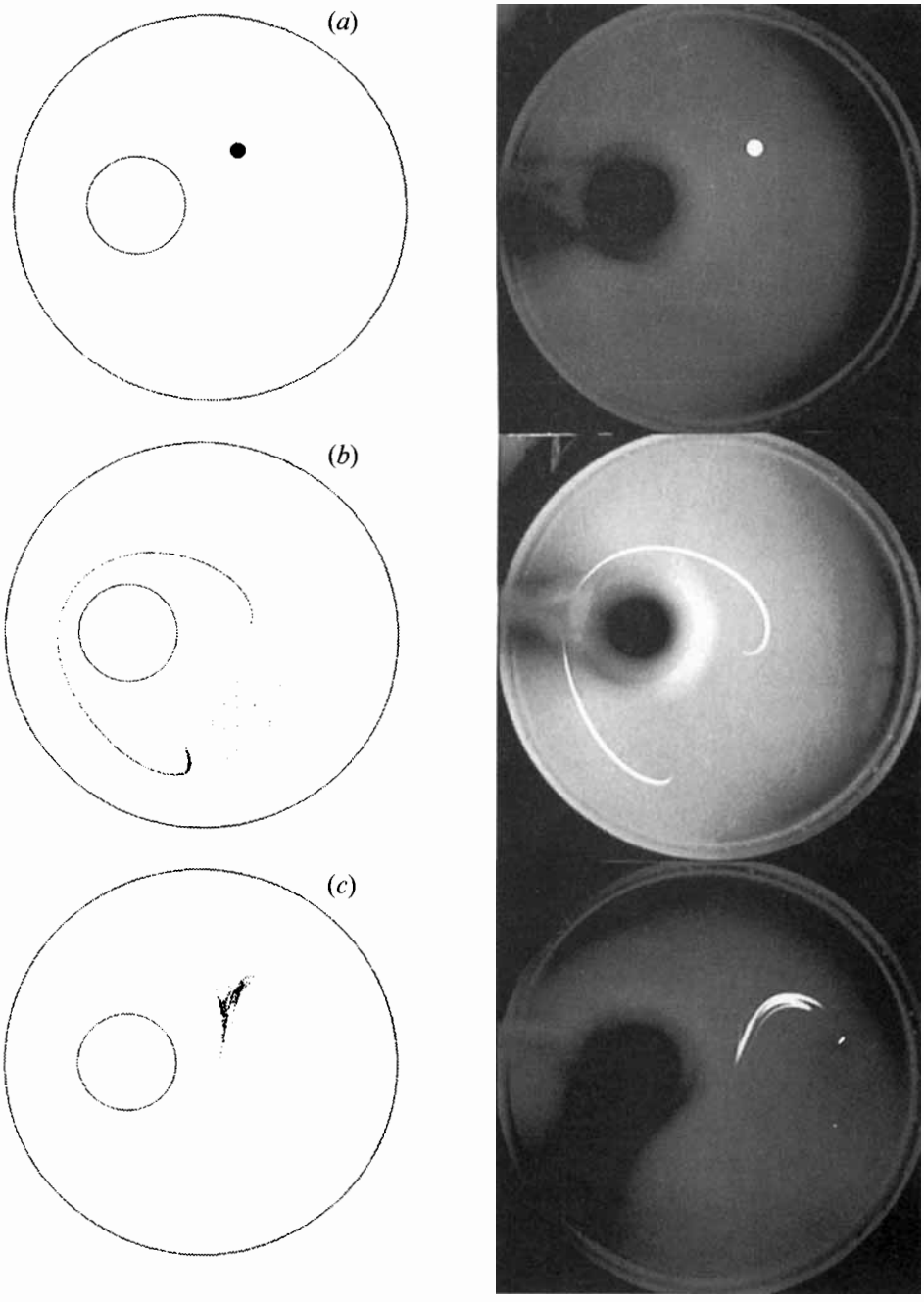

FIGURE 8. Numerical and experimental results for stirring for 7 cycles; (*a*) initial location of blob, (*b*) after 7 forward cycles, and (*c*) after flow reversal. In the numerical study, D is taken to be 5×10^{-12}.

experiments is sufficiently low. But, when we begin the reverse cycles, the initial conditions of the particles in the transient case are different from the corresponding ones produced with Stokes solution because of the 'errors' accumulated due to inertial effects during the forward cycles. These 'errors' are amplified during the course of the reverse cycles because of the sensitivity to initial conditions in a chaotic region. Figure

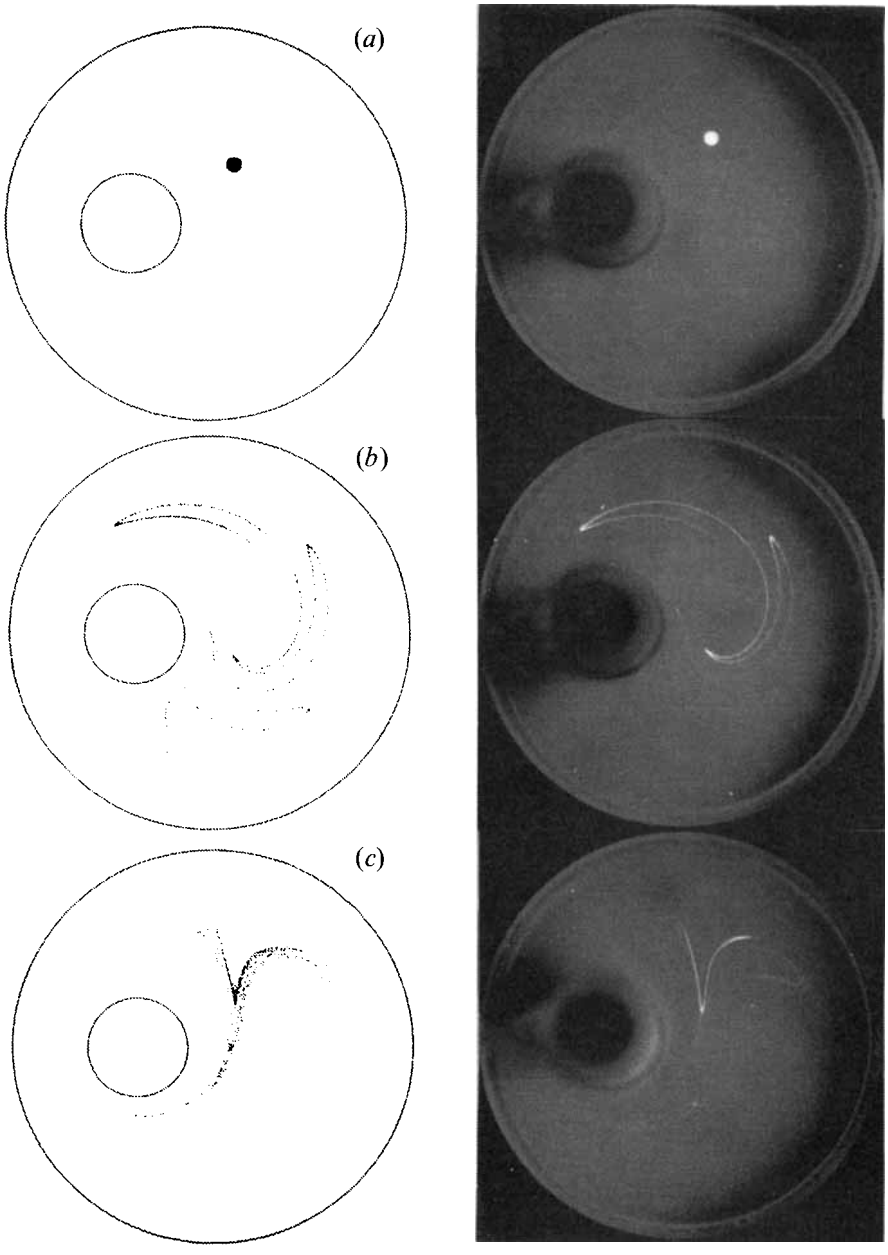

FIGURE 9. As figure 8 but for 10 cycles; (*a*) initial location of blob, (*b*) after 10 forward cycles, and (*c*) after flow reversal. In the numerical study, D is taken to be 5×10^{-12}.

8, which shows the case for 7 cycles, shows that the particles branch out at a particular location in the flow reversal picture. For the case of 10 cycles, the particles diverge in the same region (figure 9). Hence, we may expect a hyperbolic point in this neighbourhood.

Figure 10 shows the separate and combined effects of diffusion and transients on the separation of particles. It may be noticed that, for a few cycles of stirring (up to 5), the combined effect of diffusion and transients is more than the sum of the individual effects. For longer duration of stirring, however, the combined effect becomes less than

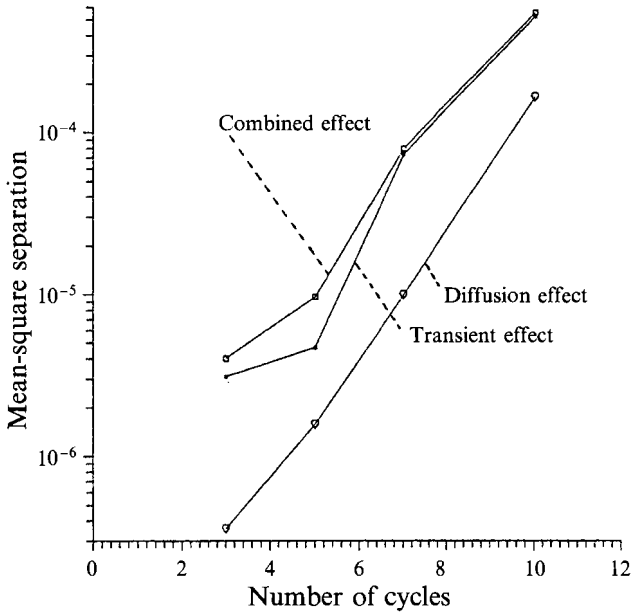

FIGURE 10. Mean-square separation with various cycles of stirring showing separate effects of diffusion and transient velocities and also their combined effects.

the sum of the individual effects, and the transient effects alone produces the bulk of the separation. Using the physical dimensions of the system, and considering that the duration of transient velocities is about 1 s in a single cycle, the displacement of a particle due to transient velocities for a cylinder rotation speed of 0.1 r.p.m. is about 10^{-4} m. Similarly, taking D to be about 10^{-12} m^2 s^{-1} and the duration of a cycle to be about 10^2 s, the characteristic displacement due to diffusion effects is estimated to be about 10^{-5} m. Thus, for a flow within the Stokes regime, the diffusion effects and the transient velocity effects are comparable in producing perturbations to the particle trajectories, so neither can be neglected while estimating the separation of particles produced in a chaotic advection. Moreover, the two processes can be thought to be acting at different times during the cycle. When transient effects are dominant (during starting, stopping, and switching of cylinder motions), diffusion has a negligible effect because the duration is too short. During the rest of the cycle, the motion is steady, thus making the transient velocities zero while allowing the diffusion process to take place over a longer time-span. This is perhaps the reason why the additive effect occurs for a few cycles of stirring. For a longer duration of stirring, however, the other nonlinear effects of stretching and folding occur, which are not taken into account in our above scale analysis. Hence, for a larger number of cycles of stirring, these effects should also be taken into account.

Since it is now evident that both molecular diffusion and inertia effects make contributions to the overall separation of particles, it may be appropriate to study their relative effects using the Péclet number, $Pe = VL/D$, where $V = \Omega R_o$ is a characteristic velocity, $L = (R_o - R_i)$ is a characteristic length of the system, and D is the molecular diffusivity. The Péclet number is varied by using different values of the diffusion coefficient, D, of 10^{-10}, 10^{-11} and 10^{-12} m^2 s^{-1}. Figure 11(a) shows the variation of mean-square separation with the duration of stirring for various Péclet numbers for the case of chaotic advection with molecular diffusion and no inertial effects. For high and

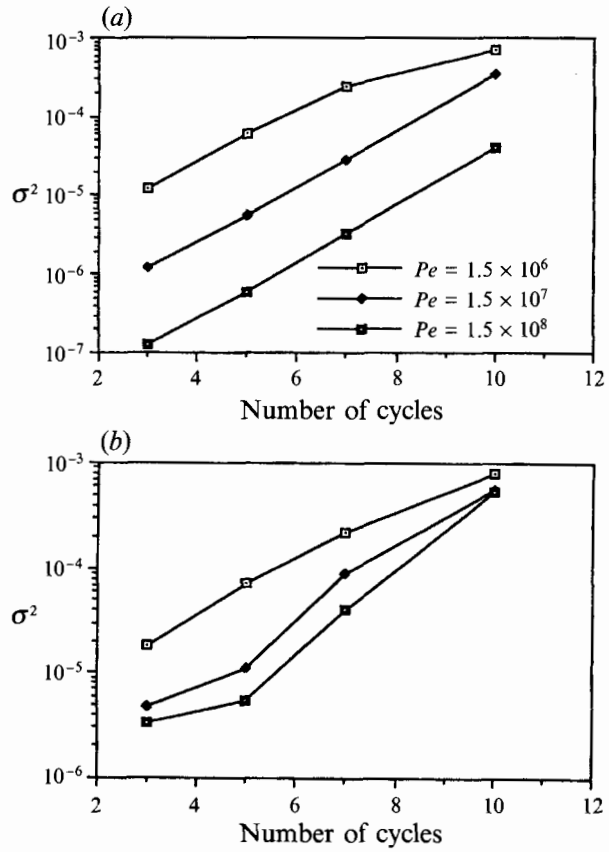

FIGURE 11. Variation of mean-square separation with the duration of stirring for various Péclet number for the case of chaotic advection with molecular diffusion and (*a*) no inertial effects, and (*b*) with inertial effects included.

medium Péclet numbers, the behaviour is similar, i.e. the separation increases almost exponentially with stirring time. For low Péclet numbers, however, the increase in separation slows down with longer duration of stirring. This phenomenon may be explained by considering the fact that there may be multiple folds of the blob when stirring takes place for a longer duration, and, if the diffusivity is sufficiently high, there is a distinct possibility that particles from one arm of the fold diffuse into an adjacent arm. When transient effects are included (figure 11*b*), the separation of particles at the larger number of cycles of stirring become less dependent on the Péclet number, indicating that the inertial effects dominate when the stirring is over a long period.

5. Conclusions

The above results show that inertial effects, in spite of their low orders of magnitude and very short duration, can play a significant role in enhancing mixing in a periodically driven flow in an eccentric annulus. This phenomenon is expected to be valid for similar flows in other geometries also. Moreover, since the particles undergoing separation in this study represent passive scalars, the concept can be used for enhancement of heat transfer as well, particularly for the case of high Prandtl number fluids.

From this study, we find that a flow solution obtained by solving the Navier–Stokes equations numerically can also be used for studying chaotic advection in an eccentric annulus. Figure 4 shows that all the structural details in a Poincaré section predicted by using an analytical solution of the velocity field can be captured very effectively by using a numerical solution of the velocity field produced by a modest mesh size with 31×61 grids. This points toward the possibility of studying chaotic advection including several realistic features such as inertia, vibration and body forces; non-Newtonian fluids could be studied in this manner as well.

The support of the work by the National Science Foundation under Grant No. CTS-89-18511 is gratefully acknowledged.

REFERENCES

AREF, H. 1984 Stirring by chaotic advection. *J. Fluid Mech.* **143**, 1.

AREF, H. & BALACHANDAR, S. 1986 Chaotic advection in a Stokes flow. *Phys. Fluids* **29**, 3515.

AREF, H. & JONES, S. W. 1989 Enhanced separation of diffusing particles by chaotic advection. *Phys. Fluids* A **1**, 470.

BALLAL, B. Y. & RIVLIN, R. S. 1977 Flow of a Newtonian/Fluid between eccentric rotating cylinders: inertial effects. *Arch. Rat. Mech. Anal.* **62**, 237.

CHAIKEN, J., CHEVRAY, R., TABOR, M. & TAN, Q. M. 1986 Experimental study of Lagrangian turbulence in a Stokes flow. *Proc. R. Soc. Lond.* A **408**, 165.

CHIEN, W.-L., RISING, H. & OTTINO, J. M. 1986 Laminar mixing and chaotic mixing in several cavity flows. *J. Fluid Mech.* **170**, 355.

CHO, C. H., CHANG, K. S. & PARK, K. H. 1982 Numerical simulation of natural convection in concentric and eccentric horizontal annuli. *Trans. ASME* **104**, 624–630.

DUTTA, P. & CHEVRAY, R. 1991 Effect of diffusion on chaotic advection in a Stokes flow. *Phys. Fluids* A **3**, 1440.

JONES, S. W. 1991 The enhancement of mixing by chaotic advection. *Phys. Fluids* A **3**, 1081.

JONES, S. W. & AREF, H. 1988 Chaotic advection in pulsed source-sink systems. *Phys. Fluids* **31**, 469.

KHAKHAR, D. V., FRANJIONE, J. G. & OTTINO, J. M. 1987 A case study of chaotic mixing in deterministic flows: the partitioned pipe mixer. *Chem. Engng Sci.* **42**, 2209.

KHAKHAR, D. V. & OTTINO, J. M. 1985 Chaotic mixing in two-dimensional flows: stretching of material lines. *Bull. Am. Phys. Soc.* **30**, 1702.

LEONG, C. W. & OTTINO, J. M. 1989 Experiments on mixing due to chaotic advection in a cavity. *J. Fluid Mech.* **209**, 463.

LIU, M. & PESKIN, R. L. 1991 Chaotic behavior of particles in 2D cavity flow. *Phys. Fluids* A **3**, 1436.

MUZZIO, F. J., MENEVEAU, C., SWANSON, P. D. & OTTINO, J. M. 1992 Scaling and multifractral properties of mixing in chaotic flows. *Phys. Fluids* **4**, 1439.

MUZZIO, F. J. & SWANSON, P. D. 1991 The statistics of stretching and stirring in chaotic flows. *Phys. Fluids* A **3**, 822.

SHUSTER, H. G. 1984 *Deterministic Chaos: An Introduction.* Weinheim: Physik-Verlag.

SWANSON, P. D. & OTTINO, J. M. 1990 A comparative computational and experimental study of chaotic mixing of viscous fluids. *J. Fluid Mech.* **213**, 227.

TAN, Q. M. 1985 Regular and chaotic trajectories in a Stokes flow. *Columbia University, Dept. of Applied Physics, Rep.* 101.

TJAHJADI, M., STONE, H. A. & OTTINO, J. M. 1992 Satellite and subsatellite formation in capillary breakup. *J. Fluid Mech.* **243**, 297.